Clays and Clay Minerals, Vol. 53, No. 3, 224–233, 2005.

MICROBIAL FORMATION OF A HALLOYSITE-LIKE MINERAL

KAZUE TAZAKI*

Department of Earth Sciences, Faculty of Science, Kanazawa University, Kakuma, Kanazawa, Ishikawa 920-1192 Japan

Abstract—Transmission electron microscopy (TEM) has been used to demonstrate the biological formation of a hollow spherical halloysite-like mineral in freshwater systems. The interaction between clays and microbes was investigated in microbial films from laboratory cultures derived from natural sediments. Optical and electron microscopic observations of cultured microbes revealed that thin clay films covered areas of the bacterial cell wall. X-ray diffraction of the thin films after 2 y of ageing showed a 7.13 Å *d* spacing, consistent with a 7 Å halloysite-like phase [$Al_2Si_2O_5(OH)_4 \cdot H_2O$]. Fourier transform infrared analysis of the thin film exhibited the characteristic adsorption bands for O–H (3651 cm^{-1}), C–H and C–N (2925, 1454 and 1420 cm^{-1}, respectively), suggesting that the phase was closely associated with adhesive organics. Observation by TEM of the thin films revealed that spherical, hollow, halloysite-like material formed on both coccus- and bacillus-type bacterial cells. Electron diffraction analysis of this material showed 2.9, 2.5, 2.2 and 1.5 Å *d* spacings. The present investigation strongly suggests that the thin film wall of the spherical halloysite-like material was associated with bacteria as a bio-organic product. This material, referred to hereafter as bio-halloysite, is further evidence for the microbially-mediated formation of clay minerals. The identity of the bacteria responsible for bio-halloysite formation is unknown, but is tentatively assigned to sulfate-reducing bacteria on the basis of morphology and the presence of reducing conditions in the microcosm at the end of the experiments.

Key Words—Bacterial Cell Wall, Electron Microscope, Halloysite, Hollow Spherical Forms, Microbial Formation.

INTRODUCTION

Soils are dynamic systems showing a variety of energy and mass fluxes and material transformations, and various models have been proposed to describe the formation of clay minerals within soils. The upper layers of a soil have high organic carbon concentrations and the organic content decreases with increasing depth in the soil. This gradient is usually thought to be due to the dominance of above-ground organic input to the carbon profile and much lower activity of organisms in the soil itself (Shoji *et al*., 1993). However, the major formation processes for clay minerals are thought to be biochemical, largely depending on high microbial activity in soils (Ueshima and Tazaki, 1998; Ueshima *et al*., 2000).

Examples of clay-biochemical interactions abound. Hanczyc *et al*. (2003) reported that montmorillonite catalyzes the polymerization of RNA from activated ribosome nucleotide and that montmorillonite accelerates the spontaneous conversion of fatty acid micelles into vesicles. Theng and Orchard (1995) discussed the physical and chemical interaction between microorganisms and soils in ecosystems. Bio-mineralization of kaolinite, nontronite and bentonite on living cells of microorganisms in natural and cultivated systems have been reported (Tazaki, 1997; Ueshima *et al*., 2000; Asada and Tazaki, 2000; Tazaki, 2000). The degree of mineralization in these examples ranged from poorly crystalline granules to well oriented crystalline solids. Polymeric substances secreted by microbial cells including the crystalline surface (*i.e.* S-) layer proteins, polysaccharides and capsules often provide nucleation sites and possibly a favorable chemical microenvironment for bio-mineral formation. Bacterial cells can act as a nucleation site for minerals (Ferris *et al*., 1986; Sara and Sleytr, 2000). Similarly, Tashiro and Tazaki (1999) showed that the layer of extracellular polymeric substances surrounding microbial cells can act as a template in the formation of Fe hydroxides. Urrutia and Beveridge (1993) suggested a cation-bridging mechanism in which multivalent metal cations complex with a functional group (*e.g.* COO–) which in turn bridges with ionic silicates to form large aggregates. Theng and Orchard (1995) also suggested that multivalent cations might have served as cation bridges in the interaction between clays and microbial extracellular polymeric substances.

In this study, natural occurrences of clay minerals in freshwater systems have been observed at nm to μm scales using electron microscopy. Laboratory cultivation experiments clarified the role of microbes in clay biomineralization. We observed that hollow spherical mineral forms became encapsulated on the active surface of the cell wall and that hollow spheres of a 7 Å halloysite-like phase, referred to hereafter as bio-halloysite, were produced by bacteria in natural freshwater-lake sediments at room temperature. We also

* E-mail address of corresponding author:
kazuet@kenroku.kanazawa-u.ac.jp
DOI: 10.1346/CCMN.2005.0530303

discuss the mechanism of formation of this phase on bacterial surfaces and suggest that this morphology develops due to either outgassing or vesicle formation. Study of these small-scale 'clay bubbles' can also contribute to a better understanding of the suggested environments for the development of the earliest forms of life, associated with bio-sedimentation on Earth.

MATERIAL AND METHODS

Sediment samples were collected from Passo Real Dam sediments, Portalegre, Brazil (Fonseca *et al.*, 2000; Tazaki and Asada, 2003). A sample of 20 g of reddish brown sediment, comprising mainly kaolinite with quartz, cristobalite and feldspar, was rinsed with distilled water ten times to remove fine particles. The washed sediments were incubated at room temperature under distilled water in a covered beaker with a glass slide oriented as shown in Figure 1. The incubation periods ranged from a few months to 2 y, during which time the pH, Eh and DO (dissolved oxygen) of the solution in the beaker were measured using an HORIBA portable inspection meter.

Microbes in the biofilms were examined with a polarizing optical and fluorescence microscope (Nikon OPTIPHOT-2 EFD3) using wet samples. Two fluorometric methods were used for bacteria counting. Samples stained with 4′,6-diamidino-2-phenylindole (DAPI) were observed through an episcopic fluorescence microscope. The DAPI stains the DNA in bacterial cells, and blue fluorescence under ultraviolet light (365 nm) indicates metabolically active bacteria. Samples stained with 0.1 mM 5-carboxyfluorescein diacetate (CFDA) were used for counting enzymatically active bacteria. These samples were incubated for microscopic observation.

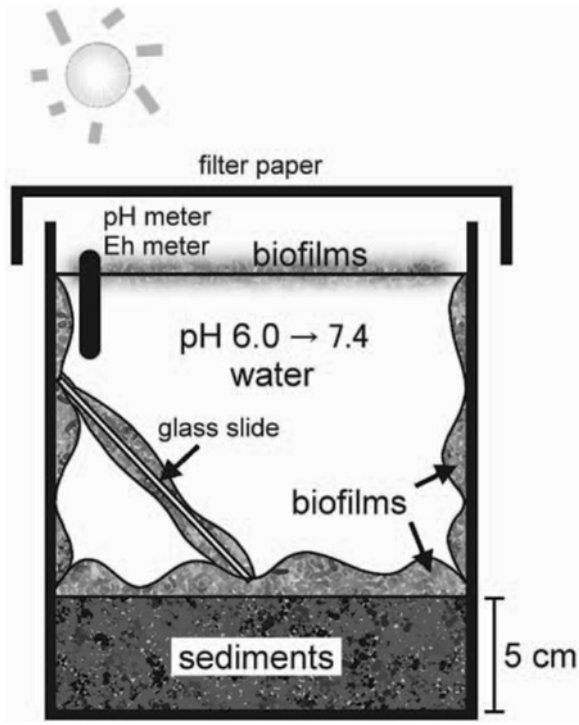

Figure 1. Schematic diagram of the simple culture system which shows the formation of biofilms on a glass slide, on the wall of a covered bottle, and on the surfaces of sediments in distilled water at pH 6–7 and in sunlight.

A low-vacuum scanning electron microscope (LV-SEM, JEOL JSM-5200LV) equipped with an energy dispersive X-ray (EDX) spectrometer (Philips EDAX PV9800EX) was used to observe the micromorphology of the bacterial surface and its chemical composition. Microbial films were mounted on stubs using carbon tape and air dried. Dehydrated samples were coated with carbon and examined at accelerating voltages of 15–25 kV.

The extracellular and intracellular conditions of the bacteria were observed using TEM (JEOL JEM-2000 EX). Electron diffraction analysis was used to identify phases present in the biofilms. One drop of the suspension was taken by pipette and mounted on the micro-grid for observation. The accelerating voltage ranged between 120 and 200 kV.

Mineralogical investigations of clay-bio-film aggregates were performed by powder X-ray diffraction (XRD). A Rigaku Rinto 1200 X-ray diffractometer (CuKα radiation) operating at 40 kV and 30 mA, and a scanning speed of 1–20 s per 0.02°2θ was used. Chemical investigations of the bio-films were carried out by X-ray fluorescence (XRF) spectroscopy using a scanning electron microscope (SEM) equipped with an energy dispersive XRF detector (ED-XRF, JEOL JSX-3201; RhKα ray). Both bio-films and powdered samples were investigated using the LV-SEM and TEM (operated at an acceleration voltage of <120 kV).

The organic compounds associated with minerals and organometallic complexes in the biofilm were analyzed by Fourier transform infrared (FTIR) absorbance spectroscopy (Jasco FT/IR-610, MICRO-20). The biofilm was air dried and ground to a fine powder; 3 μg of powdered microbial films and 10 mg of amorphous KBr were placed in a mortar, mixed thoroughly, and made into tablets using an MP-1 micro tablet maker and an MT-1 model mini-press. The FTIR analysis was then carried out on the tablets using IR frequencies between 400 and 4000 cm^{-1}.

RESULTS

Analysis of the untreated sediments (dispersed on Mylar film) by ED-XRF showed that they contained large amounts of Si, Al and Fe, with traces of Na, Mg, K, Ca, Ti and Mn. Analysis by XRD of the initial sediment showed that no halloysite-like phase was present in the untreated sediments, though it did contain kaolinite. Micromorphology by optical microscopy confirmed that

https://doi.org/10.1346/CCMN.2005.0530303 Published online by Cambridge University Press

there were no hollow spheres in the initial stage. After 2 y, the dissolved constituents in the water were analyzed by ED-XRF and contained 23 ppm Fe and 16 ppm Si associated with C, Na, Mg, Al, P, S, K and Ca ions, suggesting that some sediment dissolution and transformation had occurred.

Biofilms were observed on the glass surface after a few months, and grew to 0.01–0.1 mm thick after 1 y. Biofilms formed not only on the glass slide, beaker and top surface of the sediments, but were also apparent as an oily film on the surface of the solution (Figure 1). No biofilms grew in control samples that had been sterilized either by ultraviolet rays after boiling for 3 h or by use of ethanol instead of distilled water.

The biofilms were coated with newly formed clays after a few months' ageing at room temperature. The solution and the biofilms turned brown in color after 2 y of ageing, suggesting the precipitation of a mixture of Fe oxides and sulfides (probably Fe sulfide). A sulfide odor suggested the presence of H_2S gas in the system. The slightly reduced redox state of the solution was confirmed by Eh values of −26 mV and dissolved oxygen levels of 1.3 mg/L at pH 7.4.

Optical and fluorescence microscopic observations

After 2 y, the biofilms were mainly composed of colonies of spherical brown or greenish brown microbes associated with filamentous microbes. Optical micrographs showed abundant microbes associated with brown clay particles after 2 y of ageing (Figure 2a). The microbes fluoresced red when exposed to light of 510–560 nm wavelength, indicating that the microbes contain chlorophyll-a, which has absorption bands at 409 and 665 nm (Figure 2b). The various microbes were tentatively identified on the basis of their morphologies (Holt *et al*., 1994) as filamentous algae (1.5–2 μm wide) and spherical algae (1–10 μm in diameter), Cyanobacteria (2 μm wide), and bacteria having coccoid or bacillus morphology (<1 μm wide). The spherical cells ranged from <1 to 10 μm in diameter (Figure 2). Filamentous algae and the coccoid/bacilloid bacteria (possibly sulfate-reducing bacteria) were the primary producers of spherules. Filamentous algae produced larger spherules (Figure 2) than the coccoid/bacilloid bacteria (Figures 5 and 6), for which spherules could only be discerned by use of TEM.

XRD and ED-XRF analyses

Wet biofilms from the 2 month culture were mounted on a ceramic tile and measured as wet samples. The XRD patterns of the biofilms showed a rounded peak at 7.20 Å, suggesting the presence of 7 Å clay minerals (Figure 3, upper). On the other hand, wet biofilms from the 2 y old culture showed peaks at 7.13 Å (001), 4.43 Å (02), 3.55 Å (002), 2.49 Å (200), 2.36 Å (003), 2.22 Å (04), 1.68 Å (24) and 1.48 Å (06) (Figure 3, lower). The XRD criteria for halloysite given by Dixon (1989) were based on the relative intensities of the 0.445 Å and the 7 Å XRD reflections. The 7 Å phase in Figure 3 is kaolinite, but the morphological characteristics are consistent enough with the spherical halloysite-like phase to refer to it as 'bio-halloysite'. Traces of quartz and cristobalite were also found (Figure 3, lower). No evidence for feldspar was seen, suggesting that it had dissolved during the 2 y of ageing. The *d* spacing of the newly formed clay was the same as that of kaolin subgroup clay minerals, such as kaolinite or metahalloysite. The high background in the upper pattern suggested the presence of organic materials. The chemical and mineralogical components of the bacteria show chemical bonds with Si–O, Al–OH and organics, based on ED-XRF and FTIR data (Figures 4 and 7).

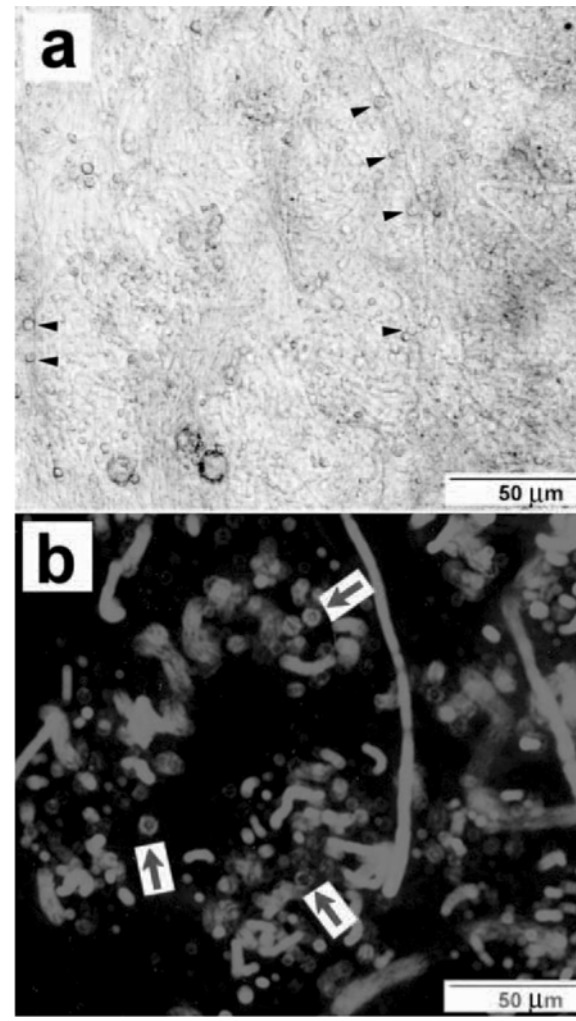

Figure 2. Optical micrographs of biofilm showing abundant microorganisms associated with clay particles. (a) Spherical materials (arrow heads) associated with filamentous algae, spherical algae, cyanobacteria and filamentous bacteria; (b) fluorescence micrograph of a DAPI-stained sample shows the red fluorescence of chlorophyll-a in spherical cells and in filamentous algae (arrows).

https://doi.org/10.1346/CCMN.2005.0530303 Published online by Cambridge University Press

Analysis by ED-XRF of the culture solution (Figure 4a) and cultured bioorganic clay (Figure 4b) indicated abundant Al, Si, S, K, Ca, Ti, Mn and Fe associated with traces of C, Mg and P. These elements might be derived from the dissolution of sediments which included feldspars. The enrichment of S and Fe over other elements is recognized in bio-halloysite-bearing biofilms. No FeS_x minerals were identified, The FeS_x minerals could be of very low crystallinity and hence undetectable by diffraction. Microorganisms, such as bacilli and cocci in the SEM images of Figure 4, are encased in exopolymeric substance. Arrows indicate broken hollow clay bubbles due to the vacuum in the SEM specimen chamber. The chemistry and *d* spacing of the halloysite-like phase obtained by SEM and XRD agreed with the electron diffraction data obtained by TEM.

LV-SEM and TEM observations

Optical micrographs of the biofilms clearly show abundant filamentous bacteria associated with spherules (Figure 2). Scanning electron micrographs of the biofilm show smaller bacteria with hollow clay spherules 1–5 μm in diameter (Figure 4 arrows). Abundant coccus- and bacillus-type bacteria were also observed on the surface of the biofilms. Chemical analysis was carried out on different parts of the biofilm. In most cases, three elements (Al, Si and Fe) were detected in the

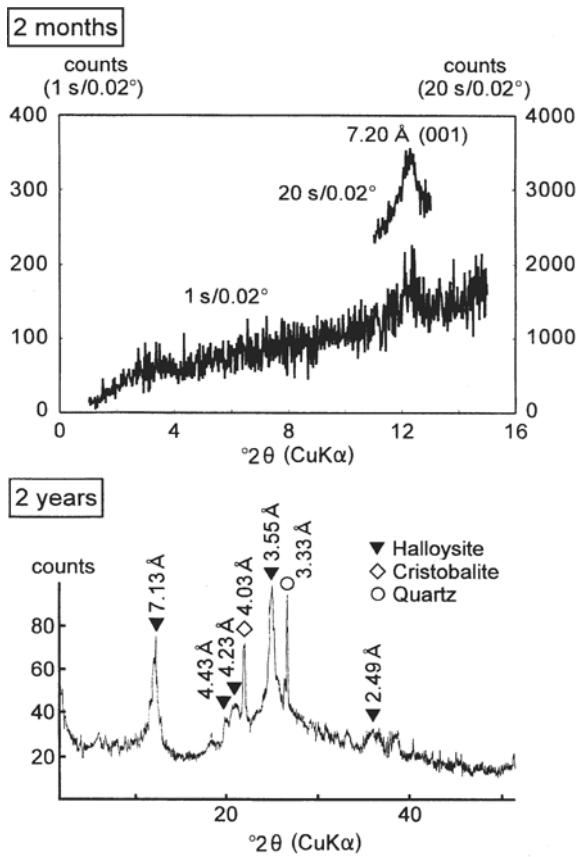

Figure 3. XRD pattern of biofilms after 2 months and after 2 y of ageing, showing the progressive crystallization of bio-halloysite.

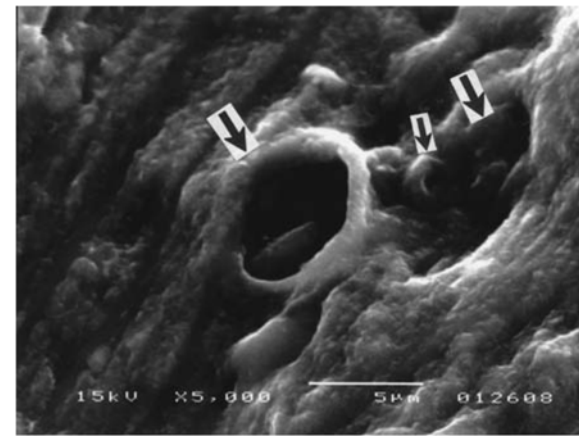

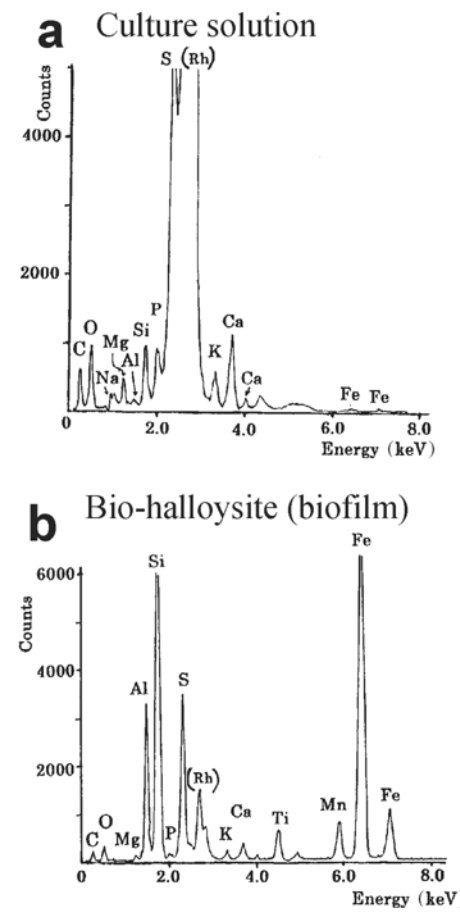

Figure 4. LV-SEM image of a bio-film with ED-XRF analyses of dried culture solution (a) and biofilm (b). The EDX spectrum of living filamentous bacteria showed major elements Al, Si, S and Fe (b). The Rh peak is due to the X-ray tube. The arrows indicate broken hollow clay bubbles, due to the vacuum in the SEM specimen chamber.

https://doi.org/10.1346/CCMN.2005.0530303 Published online by Cambridge University Press

wall of the hollow spherules, whereas additional S was detected in the bacterial cell (Figure 4b). The EDX spectra of bacteria indicated that the most abundant elements were Al, Si, S and Fe and the high background suggested the presence of organic materials, whereas EDX analyses of matrix around the bacteria showed a low background of organics.

The TEM images of hollow spherules, ~1 μm in diameter, show different stages of spherule growth, with darker marginal areas (indicating higher electron density than in the center) that strongly suggest spherical halloysite (Figures 5 and 6). These hollow spherules grew to 1−10 μm in diameter after shorter ageing times such as 2 months. The inner parts appear amorphous, nearly transparent in the TEM image (Figures 6a and b).

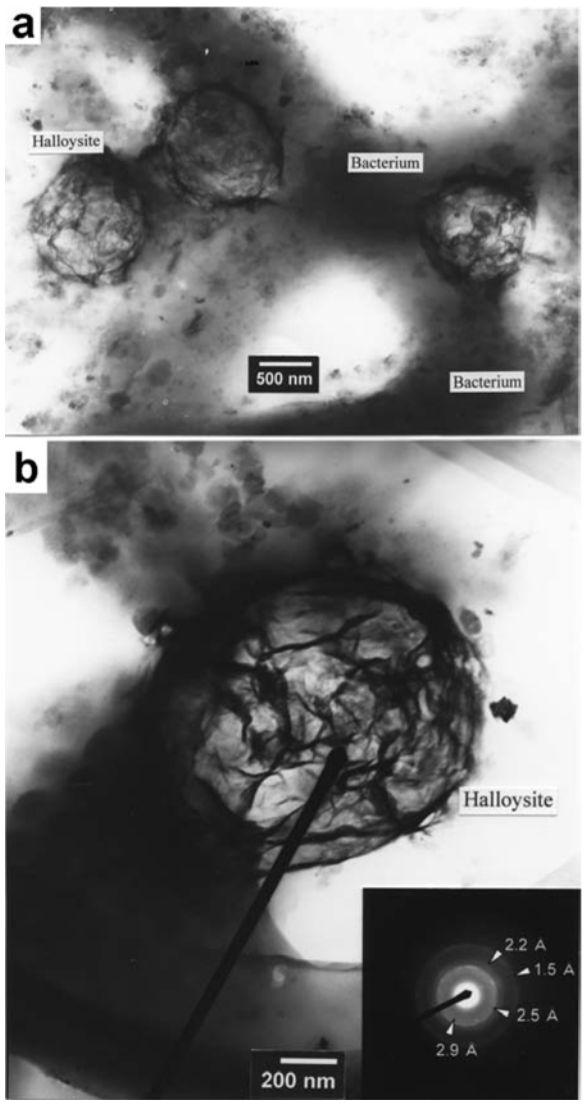

Figure 5. TEM images of bio-halloysite in clay bubbles on the surface of bacillus-type bacteria (a). The electron diffraction pattern with 2.9, 2.5, 2.2 and 1.5 Å *d* spacing also supports the suggestion of a 7 Å halloysite-like mineral (b, inset).

The thin outer skin in Figure 6a,b seems to thicken to eventually produce a dense mass of halloysite-like material as in Figures 5b and 6c. Electron diffraction spots at 2.5, 2.2 and 1.5 Å and XRD reflections at 4.43 Å (02), 2.56 Å (20), 2.49 Å (003), 2.22 Å (04), and 1.48 Å (06) are similar to those expected for 7 Å halloysite and kaolinite. The 2.9 Å *d* spacing might be

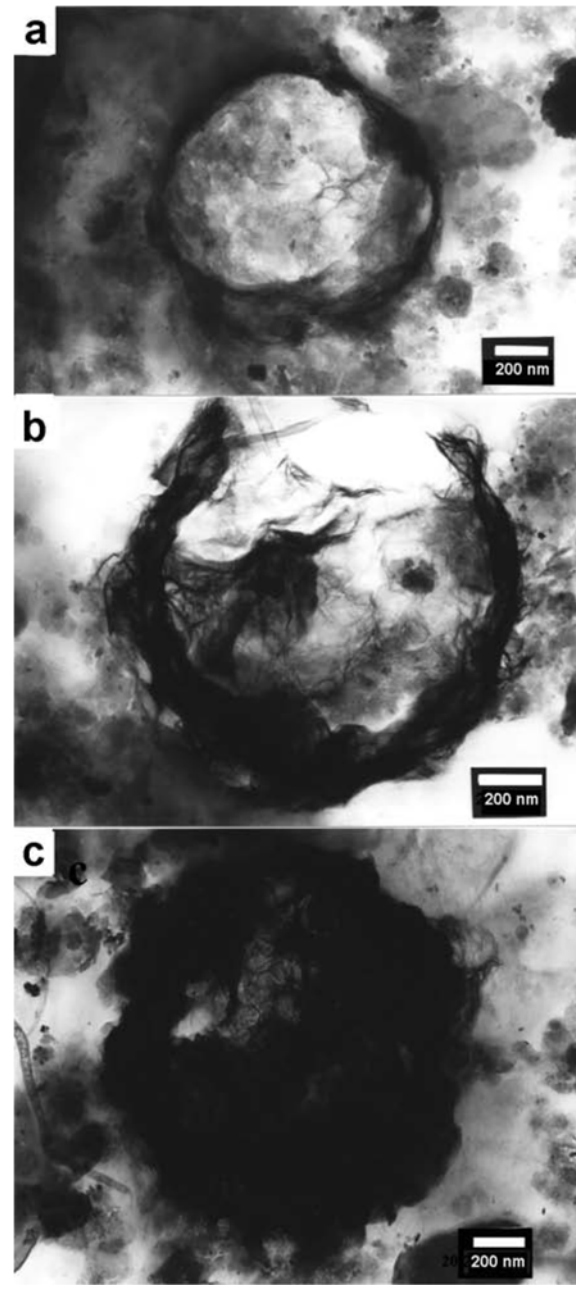

Figure 6. TEM images of the development of bio-7 Å halloysite clay bubbles. The thin wall of the bio-halloysite bubble (a) thickens to form a dense halloysite sphere (c). Some of the clay bubbles were broken out to form hollow cavities (b). The diameter increases from 800 nm to ~1 μm during ageing.

https://doi.org/10.1346/CCMN.2005.0530303 Published online by Cambridge University Press

due to the presence of maghemite 2.95 Å (220) or magnetite 2.97 Å (220), because XRF data (Figure 4) also showed high Fe content. The mineral assemblage probably contained small amounts of ferrihydrite.

Our observations revealed that the thin skin of bio-halloysite spherules thickens and eventually forms bio-halloysite spheres. Sudo and Shimoda (1978) and Sudo *et al.* (1980) have reviewed the formation of spherical halloysite in weathered volcanic ash soils in Japan. The micro-morphology and the size of spherical halloysite in their study are very similar to the bio-halloysite in this study.

The TEM observations clearly show that spherical bio-halloysite is associated with the bacteria surface (Figure 5). The development of spherical halloysite from a thin hollow sphere to a thick-walled spherical form is shown in Figure 6. Some of the hollow spheres were broken out as shown in Figure 6b. The diameter of the clay bubbles increased with ageing. Therefore, the optical micrographs collected after 2 y of ageing (Figure 2) show the clay bubbles having a minimum diameter of 5 μm, whereas TEM images collected after shorter periods of ageing, *e.g.* 2 months (Figures 5 and 6) show clay bubbles with diameters of 500 nm.

FTIR spectra

The FTIR spectrum of bio-halloysite showed a wide range of bands at 3750–3550 cm^{-1} (O–H stretch) and 1500–1300 cm^{-1} (C–N–H combination) associated with prominent absorption bands at 3697, 3622, 3405 (O–H) and 1657 cm^{-1} (H_2O). The C–H stretch (2925 cm^{-1}), Si–O stretch (1034 cm^{-1}), Al–OH stretch (912 cm^{-1}) and Si–O stretch (537 and 471 cm^{-1}) were identified as bio-halloysite (Figure 7). The most likely explanation was that the 3651 cm^{-1} absorption band was derived from bio-halloysite. The 1454 and 1420 cm^{-1} (C–N stretch) bands were also recognized as due to organics, because the standard kaolinite (API62, Cornwall, UK) did not show these bands. The other peaks were mainly from the organic matter of micro-organisms, such as N–H, C–H, C=O and C–N–H stretches derived from nucleic acids, fatty acids and polypeptides (Filip and Hermann, 2001), whereas the Si–O and Al–OH bands are derived from clay spherules.

The FTIR spectrum of bio-films showed bands characteristic of organics in contrast to the sediment samples. The absorption band at 1100 cm^{-1} was probably due to organic P–O. Either nucleic acids or cell-wall and capsular lipids containing polysaccharides could be responsible for these features. The cell proteins were typically indicated by a number of amide bands (Filip and Hermann, 2001).

Bio-halloysite has therefore been shown, by the mineralogical, chemical, and biological methods described above, to be a mixture of a 7 Å halloysite-like phase and bioorganic products.

DISCUSSION

Biomineralization of halloysite on microbes at pH 6–7

Halloysite is a common constituent in volcanic-derived soils and occurs as the dominant clay mineral in many Si-rich environments. Halloysite has a 1:1 Al:Si ratio and exhibits diverse morphologies, such as tubular and spherical forms. Most commonly, halloysite has a 10 Å basal spacing, with two interlayer water molecules per formula unit. However, halloysite is susceptible to dehydration, which leads to a 7 Å basal spacing.

In this study, bio-halloysite was successfully formed from the dissolution of kaolinite or feldspars in a cultivated biofilm after a few months and after 2 y of ageing at room temperature. Electron microscopic observations revealed that bio-halloysite grew as a thin film on the cell wall of bacillus-type bacteria. The thin films of bio-halloysite are inflated at the cell wall to

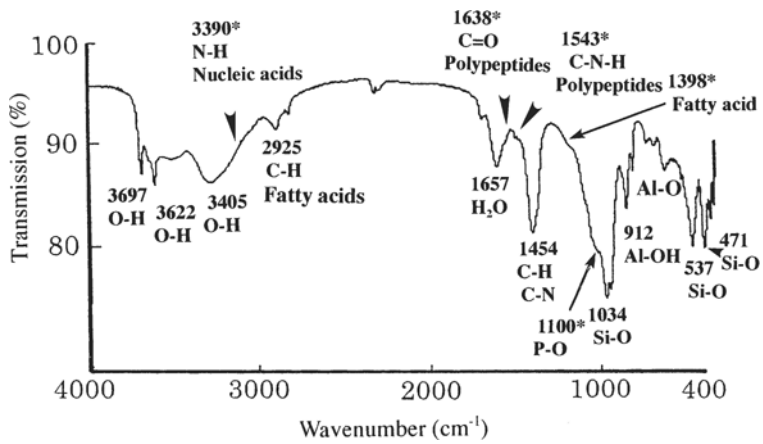

Figure 7. FTIR spectroscopy of clay bubbles in biofilms, showing not only Si–O and Al–O bands due to clay minerals, but also various kinds of organic bands, such as fatty acids, nucleic acids and polypeptides. * Possible assignments after Filip and Hermann, (2001).

https://doi.org/10.1346/CCMN.2005.0530303 Published online by Cambridge University Press

form a hollow spherical form similar to that found in volcanic ash soils.

Halloysite exhibits a wide range of structural disorders due to random stacking of structural layers. Wada and Kakuto (1985) described a poorly crystalline form of halloysite that they termed 'embryonic halloysite'. These materials showed no XRD peaks but exhibited IR absorption bands characteristic of halloysite. In this study, FTIR data of bio-halloysite showed spectral bands at 3697 and 3622 cm^{-1} suggesting the characteristic O−H bond of structural water (Tazaki and Asada, 2003). The strong bands at 2925 and 1454 are labeled as being due to C−H-stretching and bending vibrations. The presence of a mixture of OH2 and OH4 absorptions was recognized (Bish and Johnston, 1993). The absorption bands at 1454 and 1420 cm^{-1} were due to abundant organic materials in halloysite (Fialips *et al*., 2000).

Hanczye *et al*. (2003) presented experimental simulations of how clay formation may have operated and been linked with proto-life. They showed that simple physicochemical forces can drive growth and division, and that mineral particles, such as clays, can catalyze the assembly of vesicles in water. The mineral particles must have a high surface charge to be able to nucleate lipid vesicles from a solution of micelles (Russell, 2003).

The cell wall of a microbe is covered with organic adhesive material, including polysaccharides that might organize the formation of oriented clusters associated with clay particles (Ueshima and Tazaki, 2001). Kennedy *et al*. (2002) reported that organic carbon controls the orientation of mineral surfaces in black shales. Therefore, clay mineral formation by bacteria is linked to the adhesive nature of surface materials that leads to inflated spherules or 'clay bubbles'.

Comparison with spherical halloysite in volcanic soils. Spherical halloysite is often found in volcanic soils, ashes and altered pumice beds. These halloysites commonly have a high Fe content, but little or no S. For comparative purposes, a rock, consisting mainly (~90%) of K-feldspar, was collected from Ilha Bela, southern Brazil. A thick reddish rind on the rock contains well developed gibbsite and tubular halloysite (Figure 8b) formed under extreme leaching conditions (Tazaki and Fyfe, 1987a, 1987b). Energy dispersive XRF analysis of the circular materials on the K-feldspar shows that it consists of Si and Fe with small amounts of Al, K and Mn (Figure 8b, inset). Further alteration shows 7 Å lattice images and circular primitive sheet structures reminiscent of globular halloysite (Figure 8a). The Fe-rich compositions are typical of spherical halloysite (Kirkman, 1977). As shown in Figure 8b, clay precursors may well precede the formation of spherical particles of halloysite, although they have not been described as the result of biologically mediated alteration.

In the present study, a spherical halloysite-like phase, having a high S content, formed with the mediation of microorganisms under reducing conditions. The biomineralization of halloysite is correlated with sulfate reduction and H_2S gas production. Aerobic conditions are necessary for the initial breakdown of hydrocarbons and in subsequent steps, nitrate or sulfate may serve as a terminal electron acceptor (Bartha, 1986). The low Eh and dissolved oxygen values observed in this experiment suggest that reducing conditions were present and that sulfate-reducing bacteria may have played a role in the formation of bio-halloysite.

Formation mechanism of bio-halloysite. Based on the current evidence, one can only speculate as to the formation mechanism of the bio-halloysite. One such mechanism is proposed in Figure 9. It is suggested here that bacteria inflate a thin clay skin to form a vesicle through some form of degassing, probably of the O_2, CO_2 or H_2S gases which accumulated in the culture

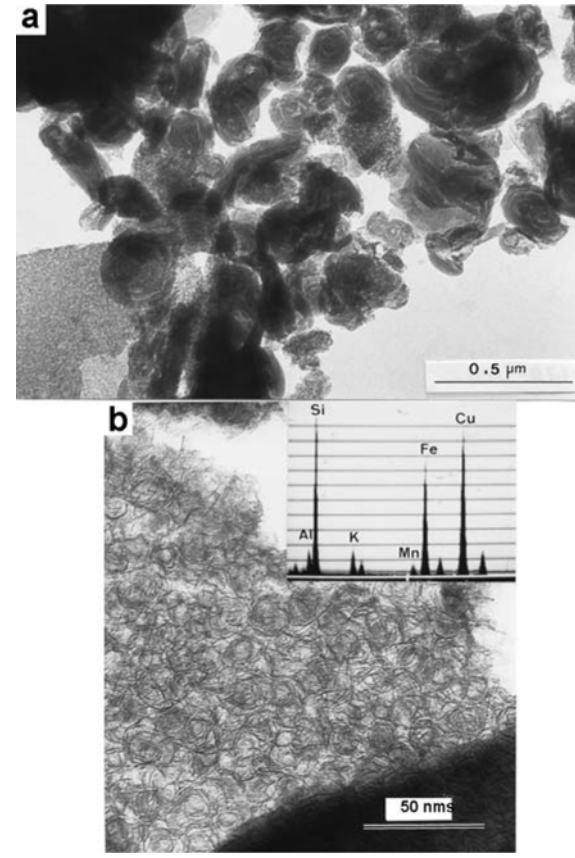

Figure 8. TEM image of the well developed spherical halloysite in volcanic ash soils from Mt. Daisen (a) and the well developed primitive clay precursors on K-feldspar (b) showing a 15−20 nm circular form and 1.4−2.0 nm lattice images. Inset in part b is an energy dispersive analysis of the material in part b which consists of Al, Si, K, Mn and Fe. The Cu peak is due to the micro grid.

https://doi.org/10.1346/CCMN.2005.0530303 Published online by Cambridge University Press

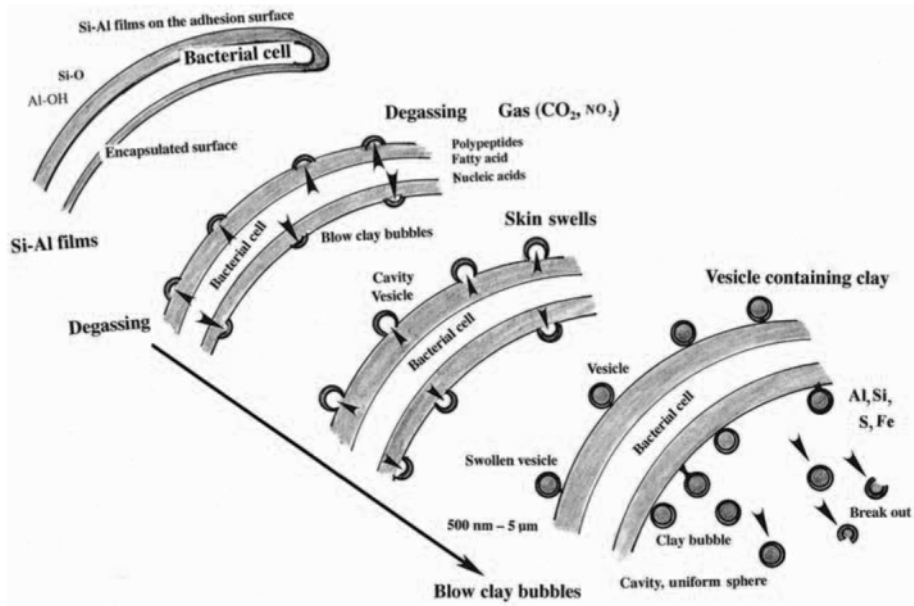

Figure 9. Schematic diagram illustrating one possible mechanism of clay-bubble bio-halloysite formation. These clay bubbles might serve as a precursor for spherical halloysite crystallization. The formation mechanism of the hollow-sphere morphology of bio-halloysite seems to be the inflation of clay bubbles by the degassing of H_2S gas into the cohesive materials of the bacterial cell wall under the low redox conditions of the solution.

solution, on the basis of morphology, the presence of reducing conditions, a high S content and the odor. If the algae or cyanobacteria are involved in the formation of bio-halloysite, then O_2, and/or CO_2 gases produce the hollow spheres. If only coccoid/bacilloidal bacteria are associated with the bio-halloysite, H_2S gas could be involved. The pH changed during the course of the experiment from 6 at the starting point to 7.4 after 2 y of ageing. The composition of the solution also changed; Al, Si and Fe all increased. H_2S gas was generated and the solution smelled of S as the redox status of the solution changed, with the Eh dropping to 0–50 mV. This suggests the presence of sulfate-reducing bacteria, as these would generate copious amounts of H_2S (g) and would precipitate Fe as a sulfide. The bacteria observed in this study facilitated the bioorganic formation of the clays. The cell walls of microbes generally include polysaccharides and proteins, and have an affinity for clay minerals. The vesicles were pushed out from the adhesion surface at the cell wall as the microbe generated and released gases. This leads to the uniform size and bubble morphology of the clay. The rate of gas generation must be constant and the cell pore size must be uniform to result in the relatively uniform size of the clay bubbles.

A contrasting model is based on the assumption that no free gas can be found in bacteria unless they have special organelles, called 'gas vesicles', to separate the gas from the fluid phase in the cytoplasm. Any gas produced internally would therefore be dissolved and would diffuse out of the cell. Gram-negative bacteria normally produce and liberate vesicles from their surface (Beveridge, 1999). No gas is necessary to 'blow' these 'bubbles' as they are naturally excised from the bacterium. The vesicles consist of outer membrane and periplasmic materials and make good nucleation sites for mineral development. Most sulfate-reducing bacteria are gram-negative bacteria.

Synthesis in NaCl brines designed to simulate crystallization of rounded particles has been demonstrated (Goldman and Stoffers, 2002). Similar rounded phases (Si/Fe = 0.26) were synthesized under saline, neutral hydrothermal conditions (40ºC, pH 7, 2 M NaCl, with initial Si/Fe = 1.5). This resulted in poorly ordered hisingerite, exhibiting a very broad XRD pattern, and having an oval morphology arranged in very fine sheets. In the present study the phase did not resemble hisingerite; instead it produced a new bio-halloysite phase suggesting the key role played by the microbes.

In this study, the laboratory experiments indicated that bio-halloysite formation in fresh water after a few months to 2 y of ageing can be ascribed to an initial crystallization of biological origin, rather than inorganic origin. Clay bubbles may have been produced initially by bacterial degassing or vesicle formation. Clay bubbles of a uniform size form intervals on the cell-wall structure (Figure 9). Some of the clay bubbles were fragile and easily broken due to the thin wall (Figures 4 and 6b). Hollow spheres developed as shown by the decreasing density from the rim to the center of the bubble. With time the thin films thicken, becoming a dense wall as shown in Figure 6c. Finally, the well crystallized halloysite-like clay bubbles (vesicles) might have been released from the bacterial surface to the

https://doi.org/10.1346/CCMN.2005.0530303 Published online by Cambridge University Press

external environment, cutting off all contact with the bacterial cell. These clay bubbles might serve as a precursor for spherical halloysite crystallization. However, it is argued here the major halloysite nucleation processes are biochemical, depending heavily on microbial activity in soils. The observation that microbial cells could mediate the formation of halloysite-like phases is a significant one that should have important consequences for soil science.

CONCLUSIONS

The TEM images clearly show the biological formation of primitive clay bubbles and the growth of a transitional product of spherical bio-halloysite. The clay bubbles, 1 μm in diameter, occurred as hollow spherical forms on the surfaces of bacterial cells. Chemical analysis of the clay bubbles indicated Al, Si, S and Fe as the major elements present. The electron diffraction pattern also identified the spheres as a halloysite-like phase. X-ray diffraction, FTIR spectroscopy, ED-XRF and SEM-EDX analytical methods used suggest that the clay bubbles did not resemble hisingerite or other clay minerals, but represented a new ordered Fe-Al silicate phase, referred to hereafter as bio-halloysite. The clay bubbles might serve as a precursor for spherical halloysite crystallization. This shows that microbial activity may play a significant role in the nucleation of clays, and that this may be a common occurrence. It is likely that the clay bubbles on the surface of bacterial cells are the bioorganic product of bacterial degassing or vesicle formation activity. Halloysite-like mineral formation in a soil may be substantially enhanced by the presence of bacteria.

ACKNOWLEDGMENTS

My thanks to Dr Jim Amonette and Dr David Dettman for their constructive comments and helpful suggestions as to how this manuscript might be improved, and to Dr Masayuki Okuno and Dr Ryuji Asada for their technical assistance. This study was partially supported by Grant-in-Aid for Science Research from the Ministry of Education, Science and Culture, Japan (Grant-in-Aid for Scientific Research B).

REFERENCES

Asada, R. and Tazaki, K. (2000) Observation of bio-kaolinite clusters. *Clay Science Japan*, **40**, 24–37.

Bartha, R. (1986) Biotechnology of petroleum pollutant biodegradation. *Microbial Ecology*, **12**, 155–172.

Beveridge, T.J. (1999) Structures of gram-negative cell walls and their derived membrane vesicles. *Journal of Bacteriology*, **181**, 4725–4733.

Bish, D.L. and Johnston, C.T. (1993) Rietveld stuctural refinement of dickite at 12 K. *Clays and Clay Minerals*, **41**, 297–304.

Dixon, J.B. (1989) Kaolin and serpentine group minerals. Pp. 467–525 in: *Minerals in Soil Environments*, 2nd edition (J.B. Dixon and S.B. Weed, editors). SSSA Book Series **1**, Soil Science Society of America, Madison, Wisconsin.

Ferris, F.G., Beveridge, T.G. and Fyfe, W.S. (1986) Iron-silica crystallite nucleation by bacteria in geothermal sediment. *Nature*, **320**, 609–611.

Fialips, C.-I., Petit, S., Decarreau, A. and Beaufort, D. (2000) Influence of synthesis pH on the kaolinite crystallinity and surface properties. *Clays and Clay Minerals*, **48**, 173–184.

Filip, Z. and Hermann, S. (2001) A attempt to differentiate *Pseudomonas* spp. and other soil bacteria by FT-IR spectroscopy. *European Journal of Soil Biology*, **37**, 137–143.

Fonseca, R., Barriga, F., Fyfe, W.S. and Tazaki, K. (2000) A geological study of bottom sediments from Passo Real and Capingui reservoirs, Rio Grande do Sul, Brazil. *Abstracts of the International Geological Congress, Rio, Brazil*, p. 235.

Goldman, N.T. and Stoffers, P. (2002) Metastable Si-Fe phases in hydrothermal sediments of Atlantis II Deep, Red Sea. *Clay Minerals*, **37**, 235–248.

Hanczyc, M.M., Fujikawa, S.M. and Szostak, J.W. (2003) Experimental models of primitive cellular compartments: Encapsulation, growth, and division. *Science*, **302**, 618–622.

Holt, J.G., Krieg, N.R., Sneath, P.H.A., Staley, J.T. and Williams, S.T. (1994) *Bergey's Manual of Determinative Bacteriology*, 9th edition. Williams & Wilkins, USA, 787 pp.

Kennedy, M.J., Pevear, D.R. and Hill, R.J. (2002) Mineral surface control of organic carbon in black shale. *Science*, **295**, 657–660.

Kirkman, J.H. (1977) Possible structure of halloysite disks and cylinders observed in some New Zealand rhyolitic tephras. *Clay Minerals*, **12**, 199–216.

Russell, M.J. (2003) The importance of being alkaline. *Science*, **302**, 580–581.

Sara, M. and Sleytr, U.B. (2000) S-layer proteins. *Journal of Bacteriology*, **182**, 859–868.

Shoji, S., Nanzyo, M. and Dahlgren, R.A. (1993) *Volcanic Ash Soils: Genesis, Properties, and Utilization*. Elsevier, Amsterdam, 288 pp.

Sudo, T. and Shimoda, S. (1978) *Clays and Clay Minerals of Japan*. Developments in Sedimentlogy, **26**. Elsevier, Amsterdam, The Netherlands, 300 pp.

Sudo, T., Shimoda, S., Yotsumoto, H. and Aida, S. (1980) *Electron Micrographs of Clay Minerals*. Kodansha, Tokyo, pp. 122-125.

Tashiro, Y. and Tazaki, K. (1999) The primitive stage of microbial mats comprising iron hydroxides. *Earth Science*, **53**, 27–35.

Tazaki, K. (1986) Observation of primitive clay precursors during microcline weathering. *Contributions to Mineralogy and Petrology*, **92**, 86–88.

Tazaki, K. (1997) Biomineralization of layer silicates and hydrated Fe/Mn oxides in microbial mats: An electron microscopical study. *Clays and Clay Minerals*, **45**, 203–212.

Tazaki, K. (2000) Formation of banded iron-manganese structures by natural microbial communities. *Clays and Clay Minerals*, **48**, 511–520.

Tazaki, K. and Asada, R. (2003) Microbes associated with clay minerals; Formation of bio-halloysite. Pp. 569–576 in: *2001. A Clay Odyssey* (E.A. Dominguez, G.R. Mas and F. Cravero, editors). Elsevier, Amsterdam, The Netherlands,.

Tazaki, K. and Fyfe, W.S. (1987a) Formation of primitive clay precursors on K-feldspar under extreme leaching conditions. *Proceedings of the International Clay Conference, Denver, 1985*, pp. 53–58.

Tazaki, K, and Fyfe, W.S. (1987b) Primitive clay precursors formed on feldspar. *Canadian Journal of Earth Science*, **24**, 506–527.

Theng, B.K.G. and Orchard, V.A. (1995) Interactions of clays with microorganisms and bacterial survival in soil: A physicochemical perspective. Pp. 123–139 in:

Environmental Impact of Soil Component Interactions (P.M. Huang, J. Berthelin, J.M. Bollag, W.B. McGill and A.L. Page, editors). CRC Press, Florida.

Ueshima, M. and Tazaki, K. (1998) Bacterial bio-weathering of K-feldspar and biotite in granite. *Clay Science Japan*, **38**, 68–82.

Ueshima, M. and Tazaki, K. (2001) Possible role of microbial polysaccharides in nontronite formation. *Clays and Clay Minerals*, **49**, 292–299.

Ueshima, U., Mogi, K. and Tazaki, K. (2000) Microbes associated with bentonite. *Clay Science Japan*, **39**, 171–183.

Urrutia, M.M. and Beveridge, T.J. (1993) Mechanism of silicate binding to the bacterial cell wall in *Bacillus subtilis*. *Journal of Bacteriology*, **175**, 1936–1945.

Wada, K. and Kakuto, Y. (1985) Embryonic halloysites in Ecuadorian soils derived from volcanic ash. *Soil Science Society of America Journal*, **49**, 1309–1318.

(*Received 12 December 2003; revised 29 December 2004; Ms. 865; A.E. James E. Amonette*)